

## A Single Stage Power Factor Correction Converter Fed VSI Based PMBLDC Motor Drive

K. Vikram Kumar<sup>1\*</sup>, P Nagaraju mandadi<sup>2</sup>, T. Anil Kumar<sup>3</sup>

### Abstract

This study introduces an innovative method to improve the effectiveness of Permanent Magnet Brushless DC Motor (PMBLDCM) systems by using a Single-Stage Power Factor Correction (PFC) converter. The suggested system employs a buck half-bridge DC-DC converter as a PFC converter to enhance power quality and regulate the voltage source inverter (VSI) that supplies PMBLDC motor. The PFC converter's front end consists of a diode bridge rectifier (DBR) that is coupled to a single-phase AC main. Therefore, the VSI functions just as an electrical switch for the PMBLDC motor, leading to energy-efficient operation. In addition, this study expands the inquiry by examining the utilization of fuzzy logic controller (FLC) in the suggested drive system. This research investigates the effectiveness of FLC in improving the performance of PMBLDC motor drives, which are often used in complex and nonlinear systems, unlike traditional applications. FLC are examined for their capacity to manage indeterminate system behaviors, hence enhancing control strategies that are more precise and dependable. The findings of the comprehensive investigation illustrate the adaptability and efficacy of FLC in enhancing the efficiency of the suggested drive system over a broad spectrum of speeds and input AC voltages. The results highlight the capability of this integrated method in attaining exceptional efficiency and energy preservation in PMBLDC motor drives.

**Keywords**— Permanent Magnet Brushless DC Motor, Single-Stage Power Factor Correction converter, buck half-bridge DC-DC converter, power quality, voltage source inverter, compressor load, air conditioner, fuzzy logic controllers.

### I. INTRODUCTION

The history of voltage controlled adjustable PMBLDC motor drives is a captivating odyssey that extends over many decades, characterized by notable milestones and scientific progress [1]. The growth of electric motor systems has been driven by the persistent quest for enhanced efficiency, accuracy, and regulation. The origin of adjustable motor drives may be traced back to the mid-20th century, coinciding with the increased need for advanced and controlled motor systems [2]. At that time, conventional electric motors were widespread, but their shortcomings in terms of speed regulation and effectiveness motivated engineers and researchers to investigate novel alternatives. The idea of Variable Frequency Drives (VFDs) [3] originated in the 1960s, establishing the foundation for motor control that may be adjusted. These first methods enabled the adjustment of motor speed by altering the frequency of the input power. Although VFDs were a notable advancement, they had several limitations, notably in terms of intricacy and the difficulties in ensuring a consistent speed under different loads [4].

Pulse Width Modulation (PWM) technology emerged as a significant advancement throughout the 1970s. This method included swiftly alternating the power supplied to the motor, so generating a fluctuating output of voltage and frequency. PWM not only resolved the problems associated with VFDs [5], but also offered a superior and more accurate method of controlling motors. This technical

---

<sup>1</sup> \* PG Scholar, Department of EEE Anurag University, Hyderabad, Telangana. kammarivikramkumar117@gmail.com,

<sup>2</sup> Assistant professor, Department of EEE Anurag University, Hyderabad, Telangana. Nagarajueee@anurag.edu.in,

<sup>3</sup> Professor and Head Department of EEE Anurag University, Hyderabad, Telangana. thalluruanil@gmail.com

advancement signaled the beginning of a new epoch in motor drive systems. During the 1980s, there was a change in attention towards the integration of sophisticated control algorithms with PWM technology. The introduction of microprocessors and digital signal processors (DSPs) [6] enabled the use of advanced control algorithms, leading to enhanced motor performance and efficiency. Engineers initiated an investigation into the capabilities of closed-loop control systems, which allow motors to adapt their functioning in real-time by using input from sensors [7].

Simultaneously, the PMBLDC motor began to acquire importance at the same timeframe. PMBLDC motors differ from standard brushed DC motors in that they have permanent magnets on the rotor, hence removing the need for brushes and commutators. This design provided intrinsic benefits such as less maintenance, enhanced efficiency, and heightened power density [8]. Integrating PMBLDC motors with modern control systems was a natural progression in the pursuit of achieving optimum motor performance. During the 1990s, there was a significant increase in the amount of research and development focused on the creation of Voltage Controlled Adjustable PMBLDC Motor Drives. These systems integrated the advantages of PWM technology [9], digital control algorithms, and the inherent benefits of PMBLDC motors.

An important issue tackled during this period was the development of reliable position and speed sensors to provide precise feedback in closed-loop control systems. Optical encoders and Hall effect sensors have emerged as dependable options, allowing accurate monitoring of rotor position and speed. This advancement greatly improved the ability to regulate and dependability of PMBLDC motor drives.

## II. LITERATURE SURVEY

Thapliyal, et al. proposed a VMC-based integrated bidirectional multi-source DC-DC converter [10]. This converter was non-isolated and developed for VSI-fed motor drives. The strategy included designing the bidirectional converter, implementing the VMC technology, and simulating its performance in VSI-fed motor drives. The bidirectional converter made energy transmission between potential sources simpler, increasing system flexibility. Drawbacks included limited experimental validation and implementation difficulties such component type modifications. Owusu, et. al optimized a Sinusoidal PWM controller in VSI-driven BLDC motors using a neural network [11]. This included building a neural network-based optimization method, integrating it with the PWM controller, and performing simulations to optimize controller performance. The neural network simplified controller parameter tuning to increase motor drive efficiency. It required a lot of training data and might have problems with real-time application.

Solar-powered position sensorless PMBLDC motor drives with dynamic observer control were suggested by Sen, Aryadip, , et al. [12]. The method included building the solar-powered drive system, creating the sensorless control algorithm, and simulating system performance. Using solar power to maintain engine energy consumption. Limitations included limited experimental validation and the necessity to adjust for real-world solar conditions. Bin, Li, and colleagues devised a power factor correction and total harmonic distortion reduction-based BLDC motor drive design technique [13]. The method included designing the power factor correction circuit, minimizing distortion, and simulating the drive's performance. Power factor adjustment improved energy economy, while distortion reduction improved motor drive performance. Due to a lack of experimental validation and practical applicability issues,

The adaptive delay-compensated position sensorless PMBLDC motor drive by Saha, Biswajit, and Bhim Singh [14] incorporated regenerative braking for Light Electric Vehicle (LEV) applications. The sensorless control method, adaptive delay compensation, and motor drive simulations were part of the approach. Sensorless control made LEV operation more cost-effective and reliable, while regenerative braking increased energy efficiency. The downsides were limited experimental validation and concerns for real-world operational conditions. Patil, et al. [15] developed a Fuzzy Logic Controller (FLC) to manage BLDC drive speed utilizing Field-Oriented manage (FOC) and Space Vector Pulse Width Modulation (SVPWM)-based VSI. For the approach, the FLC was built, combined with FOC

and SVPWM, and simulated to test the drive's speed control. The FLC enhanced speed control precision, while the FOC and SVPWM ensured motor drive efficiency. The limitations were limited experimental validation and concerns about real-world load variations. Kavin, K. S, et al. proposed a grid-interactive PMLDLC electric vehicle with a high-gain interleaved DC-DC SEPIC converter [16]. Simulating the electric car's performance required establishing the grid-interactive system, installing the high-gain interleaved converter, and performing simulations. PV integration was developed for grid-independent, sustainable operation, while the SEPIC converter improved energy efficiency. Due to a lack of experimental validation and practical applicability issues,

Through Multi-Sector SVPWM based on the Adaptive Network-Based Fuzzy Inference System (ANFIS), Kumar, Ch Vinay, G. Madhusudhana Rao, and A. Raghu Ram [17] designed a sensorless BLDC motor drive. The method included creating a sensorless control algorithm, implementing Multi-Sector SVPWM, and simulating the motor drive's sensorless operation. ANFIS promoted adaptive control, while Multi-Sector SVPWM ensured motor drive functioning. The limitations were limited experimental validation and concerns about real-world load variations.

Veeramuthulingam, et al. studied BLDC motor driving vibrations [18]. Investigations employed a model reference adaptive controller. The approach included developing the adaptive controller, analyzing motor vibrations, and simulating drive vibrations. Model reference adaptive control to reduce vibrations and improve motor drive performance. Due to a lack of experimental validation and practical applicability issues, Sliding Mode Observer (SMO)-based position sensorless BLDC motor drives with canonical switching cell converters were proposed by Saha, Biswajit, Bhim Singh, and Aryadip Sen [19] for light electric automobiles. The approach included creating the SMO-based sensorless control algorithm, including the canonical switching cell converter, and simulating motor drive performance. Switching cell converters improved drive efficiency, while SMO-based sensorless control provided accurate position estimates. The downsides were limited experimental validation and concerns for real-world operational conditions. Murugesan, et al. constructed a hardware prototype for a PSO-based PFC Cuk converter fed BLDC motor drive [20]. Developing the hardware prototype, installing a PSO-based power factor correction system, and testing the drive were part of the procedure. The PSO-based PFC improved power quality, while the Cuk converter optimized energy economy. There was limited experimental validation under various load conditions, and practical application issues were considered.

### III. PROPOSED SYSTEM MODEL

The control schematic shown in Figure 1 is an advanced system created to regulate the functioning of a PMLDLC drive. The core of this suggested system revolves on an innovative speed control technique that deviates from typical methods by substituting the customary control mechanisms for motor speed and stator current. The fundamental concept of this inventive approach involves changing the reference voltage at the DC connection, essentially considering it as an analogous reference speed for the PMLDLC motor. This deviation from standard control techniques simplifies the overall structure, reducing the need for a range of sensors specifically designed for voltage and current signals related to traditional motor control. The suggested speed control technique relies heavily on the strategic usage of rotor position data, which are acquired via Hall effect position sensors. These signals have a crucial role in creating the switching sequence for the VSI, thereby acting as an electronic commutator for the PMLDLC motor. Crucially, the need for rotor position data is only necessary at specified commutation points, which happen at regular intervals of every  $60^\circ$  electrical in the three-phase system. The precise use of rotor position signals enhances the effectiveness of the system, minimizing the need on constant input and streamlining the overall control approach.

The regulation of the DC link voltage, a crucial part of the system's functioning, is achieved by using a half-bridge buck DC-DC converter. The duty ratio (D) of this converter is a crucial parameter for managing the DC link voltage and plays a significant role in the overall management strategy. The use of MOSFETs as the switching component in the suggested PFC converter enables the achievement of high switching frequencies, which are essential for rapid and efficient management. To mitigate the

stress associated with switching, IGBTs are strategically used in the VSI bridge that supplies power to the PMBLDCM. The selection of IGBTs is determined by their ability to function at lower frequencies in comparison to the MOSFETs used in the PFC converter, hence reducing the impact of switching stress.

The PFC control system is a comprehensive technique that incorporates a current control loop embedded inside the speed control loop. By using continuous conduction mode (CCM) with average current regulation, this technique enhances the complexity of the system. The control loop begins by comparing the measured DC link voltage with a value that corresponds to the desired speed, serving as the basis for future control operations. The upgraded version replaces the typical Proportional-Integral (PI) controller with a Fuzzy Logic Controller (FLC), which introduces a more flexible and nuanced control method. The FLC controller analyzes the voltage error that arises from the comparison and generates a modulating current signal. Subsequently, the signal is amplified by multiplying it with a standardized template of the AC voltage being measured, and the resulting product is then compared with the DC current that is detected following the Diode Bridge Rectifier (DBR). The current mistake that follows is magnified and contrasted with a saw-tooth carrier wave of a constant frequency ( $f_s$ ) in a unipolar arrangement. This technique produces PWM pulses for the half-bridge converter, which allows for precise control of the PMBLDCM.

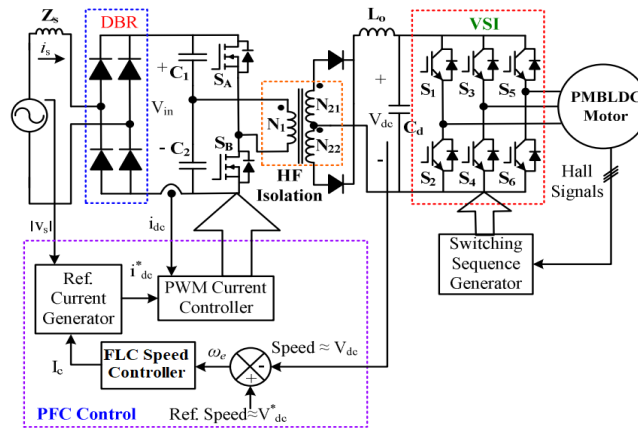


**Fig. 1.** Proposed System Model.

An notable characteristic of the suggested system is its approach to regulating current when there are sudden variations in the desired voltage, which often happens when there are modifications in the desired speed. To provide a seamless transition and avoid stator currents over the prescribed limits, a voltage gradient of less than 800 V/s is implemented for variations in the DC link voltage. This is done to guarantee that the stator currents do not exceed twice the rated current. This protective measure ensures that the stator current of the PMBLDCM stays within predetermined limits, hence enhancing the overall stability and dependability of the motor drive system.

*A. Design of PFC Buck Half-Bridge Converter Based PMBLDCM Drive*

Equation (1) is the fundamental basis for the design considerations of the proposed PFC buck half-bridge converter, which is designed for a PMBLDCM drive. This equation defines the relationship that governs the DC link voltage ( $V_{dc}$ ), which is important for maintaining power quality requirements at the AC mains and controlling the acceptable fluctuation in the DC link voltage. The equation incorporates characteristics associated with the high-frequency (HF) isolation transformer, namely  $N_1$ ,  $N_{21}$ , and  $N_{22}$ , which indicate the number of turns in the main, secondary upper, and secondary lower windings, respectively. The equation provides a correlation between the transformer parameters, namely the input voltage ( $V_{in}$ ), duty ratio ( $D$ ), and the DC link voltage.

$$V_{dc} = 2 \left( \frac{N_2}{N_1} \right) V_{in} D \text{ and } N_2 = N_{21} = N_{22}$$

Equation (2) offers a crucial understanding of how to calculate  $V_{in}$ , which is the average output of the DBR for a certain AC input voltage ( $V_s$ ). The equation incorporates a modulation factor ( $md(t)$ ), the DC link voltage ( $V_{dc}$ ), and other constants represented by  $k$ . The link between modulation, AC input voltage, and the conversion process from AC to DC is essential for understanding. It emphasizes the reliance on these components.

$$V_{in} = 2\sqrt{2}V_s/\pi$$

Equations (3) and (4) address the design of the ripple filter, a crucial element that aims to reduce the ripples in the output voltage caused by the high switching frequency of the buck half-bridge converter. Equation (3) defines the inductance ( $L_o$ ) of the ripple filter, which is intended to restrict the peak-to-peak ripple current ( $\Delta I_{Lo}$ ) of the inductor to a predetermined value for the given switching frequency ( $f_s$ ). This equation highlights the relationship between inductance, duty ratio, DC link voltage, and the required ripple limits. It provides an essential tool for building a filter that fulfills certain performance parameters. Equation (4) enhances the design by accounting for the necessary capacitance ( $C_d$ ) for the ripple filter. The calculation determines the required capacitance by considering the output current ( $I_o$ ) and the given ripple in the output voltage ( $\Delta V_{Cd}$ ). This equation offers valuable insights into how the capacitance is customized to regulate voltage fluctuations, highlighting the need of sizing the filter components to get best performance and dependability.

$$L_o = (0.5-D)V_{dc}/\{f_s(\Delta I_{Lo})\} \dots\dots\dots (3)$$

$$C_d = I_o/(2\omega\Delta V_{Cd}) \dots\dots\dots (4).$$

The subsequent narrative outlines the design parameters for the implementation, which include a base DC link voltage ( $V_{dc}$ ) of 400 V, an input voltage ( $V_{in}$ ) of 198 V from an AC source ( $V_s$ ) of 220 Vrms, and a turns ratio of the high-frequency transformer ( $N_2/N_1$ ) set at 6:1. These parameters provide a practical application of the theoretical considerations. The stated design data, including characteristics such as switching frequency ( $f_s$ ), output current ( $I_o$ ), and ripple restrictions, serve as a concrete basis for constructing and deploying the converter.

*B. Modeling of the Proposed PMBLDCM Drive*

Modeling the proposed PMBLDCM drive, which includes the PFC converter and the PMBLDCM drive, is an essential process for comprehending and forecasting the system's behavior. The integration of these two components requires the development of mathematical equations that accurately represent the dynamic interactions and reactions within each subsystem. This section provides an overview of the modeling method and emphasizes the essential mathematical expressions that together constitute the whole PMBLDCM drive. The PFC converter, an essential element of the drive, is defined by mathematical equations that precisely depict its electrical and control properties. The modeling procedure starts by depicting the converter's behavior, taking into consideration characteristics such as input voltage, duty ratio, and the transformation ratio of the high-frequency isolation transformer. A thorough comprehension of the converter's operation is achieved by considering the equations that determine the DC link voltage, modulation factors, and switching signals.

Conversely, the PMBLDCM drive, which includes the brushless DC motor and its control techniques, is represented by equations that include the motor's electromagnetic properties, rotor position sensing, and the control signals produced for commutation. The PMBLDCM drive model is built upon mathematical equations that describe the motor's torque, speed, and stator current, together with the control algorithms. The integration of these distinct models yields a comprehensive depiction of the whole PMBLDCM drive. The relationship between the PFC converter and the PMBLDCM drive is expressed by equations that illustrate how the output of the PFC converter affects the input to the motor drive, and vice versa. The interaction between these factors is essential for accurately forecasting the overall performance, efficiency, and reactivity of the integrated system.

The mathematical formulae for the PFC converter may include formulas for the modulation factor, duty ratio, and transfer functions that dictate the connection between input and output voltages. Furthermore, control loop equations, such as those for the Proportional-Integral (PI) or Fuzzy Logic Controller (FLC), have a role in determining the dynamic response of the converter. The motor model for the PMBLDCM drive incorporates equations that describe the electromotive force (EMF), torque, and the dynamics of rotor motion. These equations are often used with control techniques, such as PWM for commutation, as well as algorithms for regulating speed and current. The data acquired from sensors, such as Hall effect sensors, that determine the position of the rotor are essential for creating the sequence of switches in the inverter, which guarantees accurate commutation. To integrate these subsystem models, it is necessary to make connections between the output of the PFC converter and the input of the PMBLDCM drive. The connection between the power quality and voltage characteristics given by the PFC converter and the performance of the PMBLDCM may be fully understood via this linkage.

*C. PFC Converter*

The PFC converter is modeled by including an FLC speed controller, a reference current generator, and a PWM controller.

**FLC Speed Controller:** The Speed Controller plays a vital role in the PFC converter by regulating the speed of the Permanent Magnet Brushless DC Motor (PMBLDCM) to the necessary level. The FLC control system is used for this objective. Equation (5) presents the fundamental idea of the speed controller in the suggested control system. The speed controller, which is implemented as a Fuzzy Logic Controller (FLC), has a crucial function in ensuring that the speed of the Permanent Magnet Brushless DC Motor (PMBLDCM) remains at the required reference value. At the kth moment in time, the reference DC link voltage  $V_{dc}^*(k)$  is compared to the detected DC link voltage  $V_{dc}(k)$  to determine the voltage error  $V_e(k)$ . The error, which indicates the difference between the intended and actual DC link voltages, is used as the input to the FLC controller. The FLC controller analyzes the error and produces a control signal  $I_c(k)$  at the kth moment, considering both the proportional and integral factors.

Equation (6) presents a comprehensive formula for the output of the FLC controller,  $I_c(k)$ , at the kth moment. The iterative computation of this output considers the previous controller output  $I_c(k-1)$ , the proportional term  $K_p$  multiplied by the difference between successive voltage errors ( $V_e(k) - V_e(k-1)$ ), and the integral term  $K_i$  multiplied by the current voltage error  $V_e(k)$ .  $K_p$  and  $K_i$  represent the proportional and integral gains of the FLC controller, respectively. The proportional component highlights the instantaneous disparity between the reference and measured voltages, while the integral term aggregates the past inaccuracy, enhancing the precision under steady-state conditions.

$$V_e(k) = V_{dc}^*(k) - V_{dc}(k) \dots\dots\dots (5)$$

$$I_c(k) = I_c(k-1) + K_p \{V_e(k) - V_e(k-1)\} + K_i V_e(k)$$

The reference current generator, as described in Equation (7), is responsible for calculating the reference input current ( $i_{dc}^*$ ) for the PFC converter. The reference current is obtained directly from the output of the FLC controller,  $I_c(k)$ , and is proportionately adjusted based on the unit template of the voltage at the input AC mains, represented as  $u_{Vs}$ . This relationship represents the correlation between the speed control system and the intended input current for the PFC converter.

$$i_{dc}^* = I_c(k) u_{Vs} \dots\dots\dots (7)$$

Equation (8) specifies the voltage unit template at the input AC mains, which is represented as  $u_{Vs}$ . This template is derived by evaluating the voltage at the mains, denoted as  $v_s$ , and its amplitude  $V_{sm}$ , considering the sinusoidal characteristics of the AC mains voltage. The unit template  $u_{Vs}$  plays a

crucial role in calculating the reference input current for the PFC converter. It serves as a link between the characteristics of the AC mains voltage and the control system.

$$u_{Vs} = v_d/V_{sm}; v_d = |v_s|; v_s = V_{sm} \sin \omega t$$

**PWM Controller:** The PWM controller is responsible for generating switching signals (SA and SB) for the upper and lower switches of the PFC buck half-bridge converter. This process is described by Equation (9) and Equation (10). The reference input current, denoted as \*idc\*, is compared with its sensed counterpart, idc, in order to calculate the current error, Δidc, which is equal to the difference between \*idc\* and idc. The error is further magnified by the gain kdc and then compared to a constant frequency saw-tooth carrier waveform md(t) in unipolar switching mode. The states of the upper (SA) and lower (SB) switches are determined by the circumstances specified in Equation (9) and Equation (10). If the value of kdcΔidc exceeds that of the carrier waveform, the upper switch is activated (SA = 1). Conversely, if the value of -kdcΔidc exceeds that of the carrier waveform, the lower switch is activated (SB = 1). These conditions determine the switching logic for the MOSFETs in the PFC converter, specifying the timing for each switch to be either 'on' or 'off'.

$$\text{If } k_{dc} \Delta i_{dc} > m_d(t) \text{ then } S_A = 1 \text{ else } S_A = 0 \dots\dots\dots (9)$$

$$\text{If } -k_{dc} \Delta i_{dc} > m_d(t) \text{ then } S_B = 1 \text{ else } S_B = 0 \dots\dots\dots (10).$$

#### IV. RESULTS AND DISCUSSION



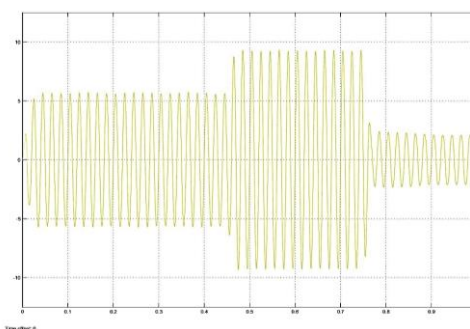
**Fig. 2.** Proposed FLC Controller Simulation Outcomes. (a) Sending Source Voltage, Vss vs Time, (b) Sending Source Current, Iss Vs Time, (c) dc Voltage Vs Time, (d) Speed, Speed reference Vs Time, (e)Torque, limiter Vs Time (f) Average Current, Vs Time, (g)Imean Vs Time.

Figure 2(a) illustrates the simulation results of the transmitting source voltage, which exhibits a sinusoidal waveform with variations ranging from -420 to +420. This value shows the electrical potential provided to the motor drive system, and the sinusoidal waveform indicates a consistent and uninterrupted flow of power. The fluctuations in amplitude may be ascribed to the control mechanisms used for voltage regulation. Figure 2(b) depicts the temporal variation of the current originating from the source, represented as a sinusoidal waveform with oscillations spanning from +10 to -10. This waveform depicts the electric current that is going from the power source to the motor drive system. The presence of a sinusoidal pattern in the data indicates that the system is exhibiting regulated and alternating current activity. The fluctuations in amplitude provide insight into the dynamic responsiveness of the system.

The results of the simulation for the direct current (DC) voltage with time may be seen in Figure 2(c). The fixed value of 420 signifies a consistent direct current voltage level throughout the system. The regular stability of the DC voltage is essential to guarantee the dependable and uninterrupted functioning of the motor drive. Figure 2(d) displays the time-dependent relationship between the speed and speed reference, illustrating the intended speed reference (1560) and the actual speed response. The congruence of the two curves demonstrates the efficacy of the control system in accurately following and sustaining the intended velocity.

The torque limitation, seen in Figure 2(e), maintains a consistent value of 11.8 throughout the duration. The torque limiter sets a maximum limit on the torque; therefore it is crucial to have a solid torque limiter to avoid excessive torque that may cause system instability. The simulation results in Figure 6.13(f) demonstrate the time-varying average current ( $I_{aa}$ ), which is represented as a sine wave with variations ranging from -9.8 to +9.8. The sinusoidal pattern indicates regulated current behavior, and the fluctuations in amplitude correspond to the system's dynamic reaction to changing load circumstances. Figure 2(g) displays the average current ( $I_{mean}$ ) as a function of time, remaining consistently at a value of 1550. This signifies a consistent and steady flow of electric current in the system, which enhances the effectiveness and regulated functioning of the motor.

The transmitting source current in Figure 3 is shown as a sinusoidal waveform with variations spanning from +5.5 to -5.5. The shown waveform illustrates the regulated and oscillating electric current that is provided to the motor drive system. The sinusoidal pattern corresponds to the anticipated response when subjected to the suggested control techniques.



**Fig. 3.** Proposed Sending Source Current.

Figure 4 illustrates the modeling results for active and reactive power over time, demonstrating a power factor of unity. The unity power factor signifies the optimal application of electrical power by the motor drive system. The constant and consistent power factor demonstrates that the recommended control mechanisms are successfully regulating the power flow in the system. Figure 5 displays the suggested stator current and EMF. The stator current is shown as a truncated sinusoidal waveform with variations spanning from +9.8 to -9.8. This waveform depicts the oscillating electric current passing through the stator windings. The electromotive force is represented as a square wave that is clipped, with variations spanning from +55 to -55. The truncated square wave pattern signifies the produced counter electromotive force in the motor, a pivotal aspect in comprehending the motor's reaction to fluctuating load situations. Figure 6 illustrates the relationship between the suggested rotor speed and time, demonstrating how the motor's rotor speed changes over a specified period. The curve illustrates the target rotor speed of 950 rpm. The congruence between the curve's alignment and the target speed serves as an indicator of the control system's efficacy in sustaining the motor speed at the designated reference point.

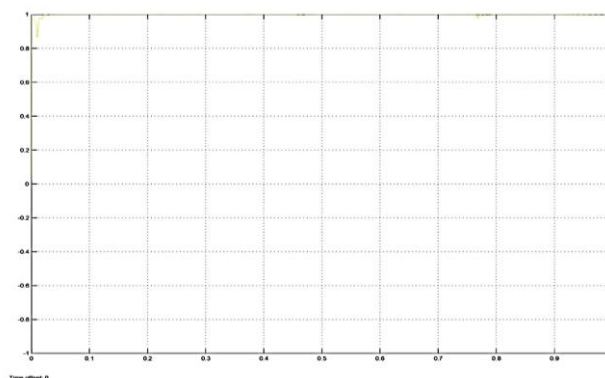


**Fig. 4.** Proposed Active and Reactive power Vs Time.

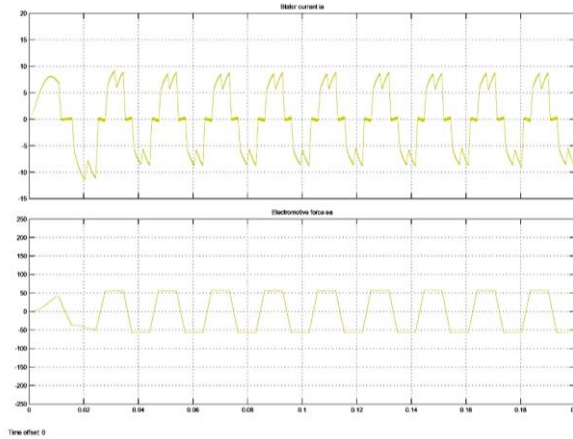


**Fig. 5.** Proposed Stator Current, and Electromotive Force.

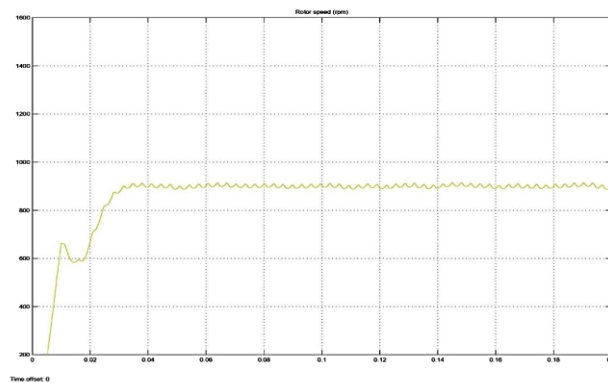


**Fig. 6.** Proposed Rotor Speed Vs Time.

Figure 7 displays the suggested electromagnetic torque as a function of time, exhibiting a fluctuation between 8 and 12 rpm. This curve depicts the torque generated by the motor and is essential for comprehending the motor's capacity to provide mechanical power. The variations in torque serve as an indication of the motor's dynamic reaction to different load circumstances.

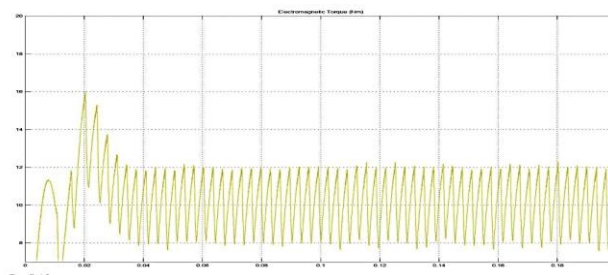


**Fig. 7.** Proposed Electromagnetic Torque Vs Time.

## V. CONCLUSION

The control scheme suggested for the Bridge-buck PFC converter fed PMBLDCM drive introduces an innovative method for controlling electric motors. This technique brings many benefits and represents notable progress in the area. The novel speed control approach, achieved by changing the reference voltage at the DC connection as an analogous reference speed, streamlines the design by substituting conventional sensor networks, therefore decreasing complexity and improving reliability. Efficient control is achieved by strategically using rotor position signals at selected commutation points, reducing the need on continuous feedback and enhancing resilience. The system achieves balance and optimization by using MOSFETs for high switching frequency in the PFC converter and IGBTs in the

VSI bridge to control the DC link voltage via a half-bridge buck DC-DC converter. The system's capacity to regulate stator current during speed variations using a rate limiter mechanism improves stability and eliminates sudden fluctuations, hence enhancing the responsiveness and dependability of the operation. Incorporating a FLC into the PFC control scheme brings flexibility to intricate and non-linear systems, hence improving the overall performance. The use of the unipolar scheme in the half-bridge converter results in reduced switching losses and enhanced efficiency during the generation of PWM pulses. The dynamic speed control system not only promotes energy saving but also coincides with current environmental concerns. The system acts as an electronic switch for the PMBLDC motor via the VSI, resulting in improved efficiency. This demonstrates a progressive approach to motor control. The use of a high switching frequency, together with meticulous component selection, effectively addresses practical factors and guarantees optimum system performance within predefined limitations.

## REFERENCES

- Doniparthi, Satish Kumar, et al. "Speed control of PMBLDC motor drive powered by solar PV array using P, PI, and PID controllers: A comparison study." *Insight-Automatic Control* 6.1 (2023): 569.
- Ammaiyappan, Bharathi Sankar, and Seyezhai Ramalingam. "Comparative analysis of two-level and three-level multilevel inverter for electric vehicle application using BLDC motor drive." *Circuit World* 49.1 (2023): 38-55.
- Malarvizhi, E., et al. "IoT Monitoring Scheme in Solar-based Motor Drive for Water Pump Applications." *2023 2nd International Conference on Edge Computing and Applications (ICECAA)*. IEEE, 2023.
- Joshua, Kanthapitchai Paul, et al. "Energy management of solar photovoltaic fed water pumping system based BLDC motor drive using NBO–SDRN approach." *Electrical Engineering* (2023): 1-15.
- Kumar, Mayank, Pankaj Deosarkar, and R. N. Mahanty. "Design And Development of BLDC Motor Drive For Solar-PV Irrigation System Using MATLAB." *2023 IEEE International Students' Conference on Electrical, Electronics and Computer Science (SCEECS)*. IEEE, 2023.
- Gowtham, V., A. Nikhitha, and S. Sashidhar. "Current Advance Angle based Rare-Earth-Free Hybrid PMa-SyRM Drive using Hall-Sensors for an Air-Conditioner Compressor." *IEEE Access* (2023).
- Shukla, Tanmay, and Srete Nikolovski. "A Solar Photovoltaic Array and Grid Source-Fed Brushless DC Motor Drive for Water-Pumping Applications." *Energies* 16.17 (2023): 6133.
- Sarode, Akash D., Shailendra Kumar, and Sanjeev Singh. "Power Quality Improvement in PMBLDC Motor Drive Using Front End Converter with Reduced Power Stages." *Recent Advances in Power Electronics and Drives: Select Proceedings of EPREC 2022*. Singapore: Springer Nature Singapore, 2023. 245-258.
- Kumar, Patnana Hema, Suresh Lakhimsetty, and Veeramraju Tirumala Somasekhar. "A low-cost fault-tolerant permanent magnet brush-less direct current motor drive for low-power electric vehicle applications." *International Journal of Circuit Theory and Applications* (2023).
- Thapliyal, Rakesh, Sourav Bose, and Prakash Dwivedi. "An Integrated Bidirectional Multi-Source DC-DC Converter with VMC Approach for VSI-Fed Motor Drive Using Non-Isolated Topology." *IEEE Transactions on Energy Conversion* (2023).
- Owusu, George, John Kojo Annan, and Solomon Nunoo. "Neural Network-Based Optimisation of Sinusoidal PWM Controller for VSI-Driven BLDC Motor." *Power Electronics and Drives* 8.1 (2023): 275-298.
- Sen, Aryadip, and Bhim Singh. "Solar Powered Position Sensor free PMBLDC Motor Drive with Dynamic Observer Control." *IEEE Journal of Emerging and Selected Topics in Industrial Electronics* (2023).

- Bin, Li, et al. "A novel approach to design of a power factor correction and total harmonic distortion reduction-based BLDC motor drive." *Frontiers in Energy Research* 10 (2023): 963889.
- Saha, Biswajit, and Bhim Singh. "An Adaptive Delay Compensated Position Sensorless PMBLDC Motor Drive with Regenerative Braking for LEV Application." *IEEE Transactions on Energy Conversion* (2023).
- Patil, Apoorva, and Sadhana Jadhav. "Fuzzy Logic Controller Implementation for BLDC Drive Speed Control Using FOC Approach and SVPWM Based VSI Technique." *2023 3rd Asian Conference on Innovation in Technology (ASIANCON)*. IEEE, 2023.
- Kavin, K. S., and P. Subha Karavelam. "PV-based grid interactive PMBLDC electric vehicle with high gain interleaved DC-DC SEPIC Converter." *IETE Journal of Research* 69.7 (2023): 4791-4805.
- Kumar, Ch Vinay, G. Madhusudhana Rao, and A. Raghu Ram. "Sensor Less BLDC Motor Drive Using a Multi-Sector Space Vector PWM Method Based on Adaptive Network-Based Fuzzy Inference System." *International Journal of Intelligent Systems and Applications in Engineering* 12.7s (2024): 07-19.
- Veeramuthulingam, N., A. Ezhilarasi, and M. Ramaswamy. "Vibration analysis of BLDC motor drive employing model reference adaptive controller." *International Journal of System Assurance Engineering and Management* (2023): 1-16.
- Saha, Biswajit, Bhim Singh, and Aryadip Sen. "SMO based position sensorless BLDC motor drive employing canonical switching cell converter for light electric vehicle." *IEEE Transactions on Industry Applications* (2023).
- Murugesan, Ramasubramanian, and Thirumarimurugan Marimuthu. "Hardware prototype model for PSO based PFC Cuk converter fed BLDC motor drive." *AIP Conference Proceedings*. Vol. 2764. No. 1. AIP Publishing, 2023.